Supporting Information

Rick et al. 10.1073/pnas.1222355110

SI Text

Cell Volume Determination. Cell volume of BPH-1 and WPMY-1 cells was estimated by measuring the intracellular water space by the method described by Kletzien et al. (1), as modified by Bender and Norenberg (2). Briefly, 1 mM 3-*O*-methylglucose (3-OMG) and 0.5 μCi/mL 3-[^{3}H]OMG were added to the culture 6 h before the volume assay. At the end of the incubation period, culture medium was aspirated, and an aliquot was saved for radioactivity determination. Cells were washed rapidly six times with ice-cold buffer containing 229 mM sucrose, 1 mM Tris·nitrate, 0.5 mM calcium nitrate, and 0.1 mM phloretin, at pH 7.4. Cells were harvested into 0.5 mL of 1 M sodium hydroxide. Radioactivity in the cell extracts and media was determined, and an aliquot of the cell extract was used for protein estimation with the Bio-Rad bicinchoninic acid kit. Values were normalized to protein level and cell volume was expressed as microliters per milligram protein.

Three-Dimensional Cell Size Imaging. After treatment with 10 μM gastrin-releasing peptide (GRP) antagonist for 6 h, BPH-1 and WPMY-1 cells were rinsed three times in 0.1 M PBS (pH 7.40), followed by fixation in cold methanol for 10 min. In our preliminary studies, cell shrinkage and cytoskeletal disruption was detected when primary cultures or cell lines were fixed with traditional fixatives such as formalin and acetone for longer period (for >25 min). However, no change in basal cell size was noted in our study when cells were fixed in cold methanol or formalin for 10 min. Although formaldehyde is a good choice for most immunohistochemistry/immunocytochemistry applications, we found intense staining with GRP-R antibody when these cells were fixed with methanol for 10 min without any artifact compared with the effect of formalin fixation. Cells were blocked with 10% BSA and 0.1% Triton X-100 and incubated overnight at 4 °C with Santa Cruz (sc-26836) goat anti-GRP-R at a 1:400 dilution. After exposure of membranes to Alexa Fluor 488 (A-11055) donkey anti-goat FITC at 1:500 for 60 min, cells were mounted with commercial mounting media (Vector Labs) containing DAPI (nuclear stain). Immunofluorescent images were acquired with a Zeiss LSM510/UV Axiovert 200M confocal microscope with a Plan Apochromat 40× objective lens, and a 2× zoom. Cross-sectional images were obtained at the desired *X*–*Y*, *Y*–*Z*, or *X*–*Z* coordinates from *z* stacks. Random collection of images from control and drug-treated cells was achieved by systematically capturing each image in a blinded manner by moving the microscope stage ∼5 mm in four different directions. At least 15 fluorescent images (1,024 × 1,024 resolution; step size, 5 μm) were captured per group, and the pixel volumes of these images were analyzed for cell size using Volocity 3D Image analysis software (Volocity 6.0 High Performance 3D Cellular Imaging Software Suite; PerkinElmer). Size exclusion was applied before analysis of substrate from false objects. Cell size was expressed in cubic micrometers.

Quantitative Evaluation of Cell Proliferation and Apoptosis in Rat Prostatic Epithelium. Slices of 5-μm thickness made from representative blocks of paraffin-embedded tissues were mounted on glass slides and stained with H&E for morphological analysis. The mitotic and apoptotic cells in the ventral prostate from three animals in each group were counted in 10 random fields at 40× objective magnification from three different individual ventral prostate sections. Because the size of the glands and the height of epithelial cells vary, the counts were standardized as follows: (*i*) the area of epithelium in each field was determined by using a microscope ocular net, and the crossing points of the net that coincided with epithelial cells were counted; (*ii*) the ratio of these points to the number of all points represented the percentage area of epithelia in the fields; (*iii*) the numbers of mitotic and apoptotic cells in a theoretical microscopic view field composed entirely of epithelial cells were calculated.

Total DNA Isolation. To quantify the cellular content of rat prostates, total DNA was prepared from 20 mg of ventral prostate tissue for each sample using the DNeasy Blood and Tissue kit (Qiagen). Three samples per group were analyzed. The yield and purity of DNA were determined according to the manufacturer's instructions.

Total RNA Isolation and cDNA Synthesis. Total RNA was isolated from BPH-1 and WPMY-1 cell lysates, as well as from 30 mg of prostate tissue for each sample using the NucleoSpin kit (Macherey-Nagel). Three prostate samples per group were analyzed. Quality control of RNA samples was as described (3). Two micrograms of RNA with a final volume of 40 μL were reverse transcribed into cDNA with the QuantiTect Reverse Transcription Kit (Qiagen) using Veriti 96-well thermal cycler (Applied Biosystems).

Real-Time RT-PCR. We evaluated the mRNA expression of human and rat GRP-R, neuromedin B receptor (NMB-R), bombesin-like receptor 3 (BRS-3), GRP, NMB, and Hprt1. Sequences for forward and reverse specific primers and thermal cycling conditions are shown in Table S6. Hprt1 was used to normalize for differences in RNA input. All real-time PCRs were performed in the iCycler iQ Real-Time PCR Detection System (Bio-Rad). Thermal cycling conditions for all genes were as follows: the mRNA expression was evaluated in 25-μL reaction volume containing 1× iQ SYBR green Supermix (Bio-Rad), 2 μL of cDNA, and 200 nM of specific primers. Triplicate samples were denatured at 95 °C for 3 min followed by 40 cycles at 95 °C for 15 s each and at the corresponding annealing temperature for 30 s, as previously described in detail (4). The efficiencies of all primers (Invitrogen Life Technologies) were tested before the experiments, and they were all efficient in the range of 95–105%. Negative samples were run in each reaction consisting of no-RNA in reverse transcriptase reaction and no-cDNA in PCR. Six microliters of each amplification reaction were electrophoretically separated and visualized using FlashGel DNA System (Lonza).

Rat Growth Factor, Inflammatory Cytokines/Receptors, Inflammatory Response and Autoimmunity, and Signal Transduction Real-Time PCR Arrays. Rat Growth Factor (PARN-041), Inflammatory Cytokines and Receptors (PARN-011A), Inflammatory Response and Autoimmunity (PARN-077Z), and Signal Transduction Pathway Finder (PARN-014A) RT2 Profiler Real-Time PCR arrays (Qiagen) were used to examine the mRNA levels of 336 genes related to growth, inflammatory response, and signal transduction. Total RNA extraction was as described above. Quality control of RNA samples, synthesis of cDNA, and its amplification by real-time RT-PCR arrays were performed according to the manufacturer's instructions (SABiosciences). Data analysis of gene expression was performed using Excel-based PCR Array Data Analysis Software provided by manufacturer (Qiagen). Fold changes in gene expression were calculated using the ΔΔCt method (5), and five stably expressed housekeeping genes (β_2-microglobulin, hypoxanthine phosphoribosyltransferase 1,

ribosomal protein L13a, GAPDH, and β-actin) were used for normalization of the results.

Cell Viability Assay (MTS Assay). Cell viability was determined by using the 3-(4,5-dimethylthiazol-2-yl)-5-(3-carboxymethoxyphenyl)-2-(4-sulfophenyl)-2*H*-tetrazolium (MTS) assay kit (CellTiter 96 Aqueous One Solution Cell Proliferation Assay; Promega) according to the manufacturer's instructions. Briefly, cells were seeded into 96-multiwell plates (Becton Dickinson) at a density of 5×10^3 cells per well in 100 μL of culture medium. After 24 h of incubation, the medium was replaced with fresh medium containing 0.1–10 μM RC-3940-II and then incubated for 72 h. Finally, 20 μL of MTS solution was added to each well and incubated for an additional 2 h. Mitochondrial dehydrogenase enzymes of viable cells converted MTS tetrazolium into a colored formazan product. The optical density of samples was measured at 550 nm using Victor^3 Plate reader (Perkin-Elmer). Experiments were performed in sextuplicate and repeated three times.

Cell Cycle Analysis. BPH-1 and WPMY-1 cells were grown for 24 h in 25-mL flasks at a density of 2×10^5/mL cells. On the following day, the medium was replaced with serum reduced McCoy's medium containing 0.5% serum, with or without the addition of BN/GRP antagonist RC-3940-II at a concentration of 5 μM. After 24 h of incubation, cultures were washed with PBS and covered with 1 mL of hypotonic propidium iodide/sodium citrate staining solution containing 0.3 μg/mL of Nonidet-40 detergent. A rubber policeman was used to scrape the monolayer, and vigorous pipetting was used to isolate the stained nuclei. The nuclear suspension was transferred to 2-mL tubes for analysis on a Coulter XL flow cytometer using excitation at 488 nm for generation of DNA distribution histograms. Dot plots of peak versus area of nuclei stained with propidium iodide were used for doublet discrimination. List mode data collected on forward and side scatter and DNA content of 10,000 cells were used for generation of DNA histograms and cell cycle distribution analysis by the ModFit Program (Verity Software House). Staining with isotonic propidium iodide (25 μg/mL) in normal saline was used for detection of cells with damaged membrane, which were presumed to be nonviable.

Western Blot. Prostate tissue was homogenized, and protein was isolated with the NucleoSpin Kit (Macherey-Nagel) and sonicated. Protein lysates were adjusted to equal concentrations. Western blot analyses were as extensively described (4). Primary antibodies for GRP-R (sc-26836), PCNA (sc-25280), COX-2 (4842S) (Cell Signaling Technology), androgen receptor (AR) (sc-13062), and β-actin (sc-47778) were purchased from Santa Cruz Biotechnology. The relative intensity of phosphorylated NF-κβ/p50 (pNF-κβ/p50; sc-33022) was calculated by dividing its absolute signal intensity by that of NF-κβ/p50 (sc-7178) (Santa Cruz Biotechnology). The immunoreactive bands were visualized with the Odyssey Infrared Imaging System. Version 3.0 software was used (LI-COR Biosciences).

Receptor Assays. Binding characteristics of receptors for BN/GRP were determined by analyzing binding of ^{125}I-labeled [Tyr^4]BN to tumor membrane homogenates of control mice as described (6). This radioligand can identify functional subtype 1 GRP receptors (7). The LIGAND PC computerized curve-fitting program was used to determine the type of binding, the maximal binding capacity of the receptors, and the dissociation constant.

Statistical Analysis. For statistical evaluation, SigmaStat 3.0 software (Sytat Software) was used. Results are expressed as means ± SEM. One-way ANOVA followed by Bonferroni *t* test, Student–Newman–Keuls test, or a two-tailed Student *t* test was used where appropriate, and significance was accepted at $P < 0.05$.

1. Kletzien RF, Pariza MW, Becker JE, Potter VR (1975) A method using 3-O-methyl-D-glucose and phloretin for the determination of intracellular water space of cells in monolayer culture. *Anal Biochem* 68(2):537–544.
2. Bender AS, Norenberg MD (1998) Effect of benzodiazepines and neurosteroids on ammonia-induced swelling in cultured astrocytes. *J Neurosci Res* 54(5):673–680.
3. Rick FG, et al. (2011) LHRH antagonist Cetrorelix reduces prostate size and gene expression of proinflammatory cytokines and growth factors in a rat model of benign prostatic hyperplasia. *Prostate* 71(7):736–747.
4. Rick FG, et al. (2012) Antagonists of growth hormone-releasing hormone inhibit growth of androgen-independent prostate cancer through inactivation of ERK and Akt kinases. *Proc Natl Acad Sci USA* 109(5):1655–1660.
5. Vandesompele J, et al. (2002) Accurate normalization of real-time quantitative RT-PCR data by geometric averaging of multiple internal control genes. *Genome Biol* 3(7): RESEARCH0034.
6. Halmos G, Wittliff JL, Schally AV (1995) Characterization of bombesin/gastrin-releasing peptide receptors in human breast cancer and their relationship to steroid receptor expression. *Cancer Res* 55(2):280–287.
7. Szepeshazi K, Schally AV, Treszl A, Seitz S, Halmos G (2008) Therapy of experimental hepatic cancers with cytotoxic peptide analogs targeted to receptors for luteinizing hormone-releasing hormone, somatostatin or bombesin. *Anticancer Drugs* 19(4): 349–358.

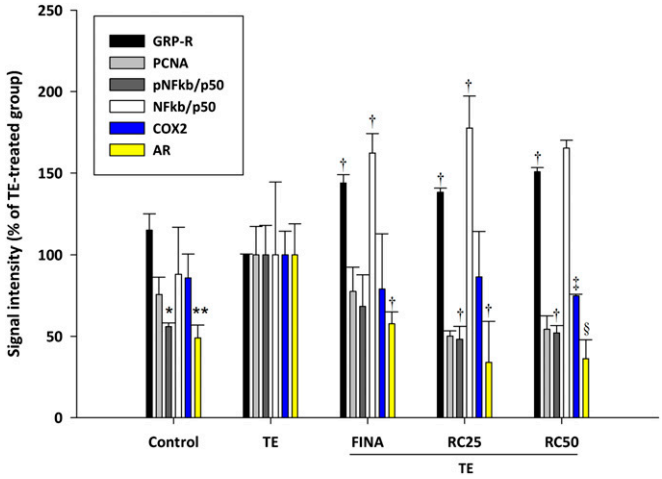

Fig. S1. Protein expression of GRP-R, PCNA, pNF-κβ/p50, NF-κβ/p50, COX-2, and AR in rat prostates ($n = 3$ in each study group) obtained by Western blotting. Signal intensity values are compared with control [$^{*}P < 0.05$, $^{**}P < 0.01$, and $^{***}P < 0.01$ compared with testosterone-enanthate (TE); $^{\dagger}P < 0.05$, $^{\ddagger}P < 0.01$, and $^{\S}P < 0.001$ compared with control by Student *t* test].

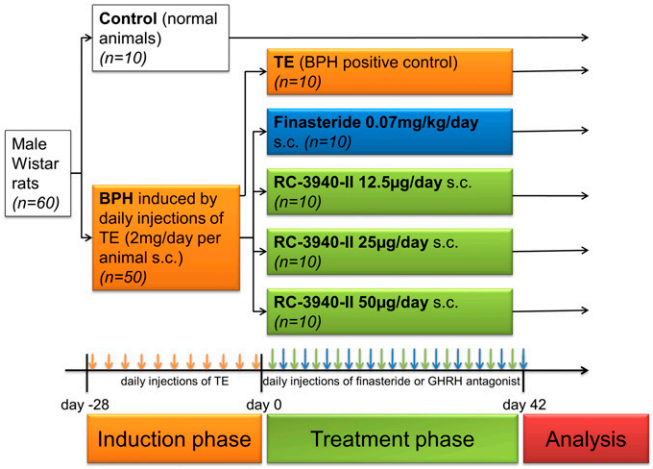

Fig. S2. Scheme of in vivo study. Induction phase included daily injections of 2 mg of TE s.c. for 28 d. In the treatment phase, 5-ARI finasteride (0.07 $mg \cdot kg^{-1} \cdot d^{-1}$), and GRP antagonist RC-3940-II at doses of 12.5, 25, and 50 μg/d were administered s.c. After 42 d of treatment, animals were killed, and prostate samples were histologically and biochemically analyzed.

Table S1. Binding characteristics of GRP receptors in control rat prostates and BPH-1 and WPMY-1 human prostatic cells

Source	B_{max}, fmol/mg membrane protein	K_d, nM
Rat prostates	417.0 ± 40.4	6.89 ± 0.13
BPH-1 cells	504.5 ± 8.5	11.21 ± 0.14
WPMY-1 cells	550.0 ± 39.0	6.24 ± 0.12

The concentrations (maximal binding capacity: B_{max}) of GRP receptors and the binding affinity (dissociation constant: K_d) were determined by radioligand binding assays. The values are means ± SE. Two to three binding experiments were done in duplicate or triplicate.

Table S2. The effect of 10 μM GRP antagonist RC-3940-II on the volume of BPH-1 and WPMY-1 cells after 6 h of exposure

	Intracellular volume measurement, μL/mg protein (decrease in % vs. control)		3D fluorescent microscopy, μm^3 (decrease in % vs. control)	
Treatment	BPH-1	WPMY-1	BPH-1	WPMY-1
Control	6.04 ± 0.64	0.92 ± 0.03	3,063 ± 139	3,185 ± 201
RC-3940-II (10 μM)	4.77 ± 0.56* (20.9)	0.72 ± 0.02* (21.7)	2,589 ± 89* (15.5)	2,688 ± 80* (15.6)

Cell volume was approximated by measuring the intracellular water space, normalized to protein level and expressed as microliters per milligram of protein, or determined by 3D image analysis with a Zeiss LSM510/UV Axiovert 200M laser confocal microscope using cell membrane GRP-receptor antibody. *$P < 0.05$ compared with control.

Table S3. Gene expression of growth factors in rat prostates after treatment with TE, TE and finasteride, or BN/GRP antagonist RC-3940-II

Gene	Accession no.	Description	Fold change			
			TE vs. control	TE/finasteride (0.07 mg/kg) vs. TE	TE/RC-3940-II (25 μg/d) vs. TE	TE/RC-3940-II (50 μg/d) vs. TE
Bmp1	NM_031323	Bone morphogenetic protein 1	**1.70**	**1.97**	−1.01	**−1.70**
Bmp10	NM_001031824	Bone morphogenetic protein 10	**1.68**	1.37	−1.32	1.04
Bmp3	NM_017105	Bone morphogenetic protein 3	**3.49**	1.11	**−2.06**	**−5.38**
Bmp4	NM_012827	Bone morphogenetic protein 4	**2.32**	**−1.97**	1.06	**−1.90**
Bmp5	NM_001108168	Bone morphogenetic protein 5	**−2.90**	1.37	−1.32	**−2.64**
Csf3	NM_017104	Colony-stimulating factor 3 (granulocyte)	**3.71**	**−2.08**	−1.07	**−7.51**
Ereg	NM_021689	Epiregulin	**2.70**	**−6.17**	1.47	**−4.56**
Fgf11	NM_130816	Fibroblast growth factor 11	**2.12**	**−1.52**	−1.06	**−1.88**
Fgf18	NM_019199	Fibroblast growth factor 18	**2.87**	**−2.37**	**−5.91**	**−3.97**
Fgf22	NM_130751	Fibroblast growth factor 22	1.38	1.46	−1.04	**−1.88**
Fgf3	NM_130817	Fibroblast growth factor 3	**5.59**	**−3.19**	−1.10	**−2.94**
Fgf5	NM_022211	Fibroblast growth factor 5	**4.70**	**−5.56**	**−1.47**	**−11.38**
Fgf7	NM_022182	Fibroblast growth factor 7	−1.26	**2.44**	−1.00	1.17
Fgf8	NM_133286	Fibroblast growth factor 8	**5.40**	1.47	−1.47	**−12.11**
Figf	NM_031761	c-fos–induced growth factor	**1.99**	**−5.72**	**−3.61**	**−3.58**
Gdf5	XM_001066344	Growth differentiation factor 5	**1.68**	1.37	−1.32	**−2.64**
Mstn	NM_019151	Myostatin	1.38	**−2.42**	**−4.38**	**−8.74**
Hgf	NM_017017	Hepatocyte growth factor	**14.25**	**−3.33**	−1.42	**−2.55**
Igf1	NM_178866	Insulin-like growth factor 1	1.15	**−2.26**	−1.40	**−1.71**
Igf2	NM_031511	Insulin-like growth factor 2	**2.21**	**−3.13**	**−6.29**	−1.14
Il11	NM_133519	Interleukin 11	**8.59**	−1.14	**−2.18**	**−2.80**
Il12a	NM_053390	Interleukin 12a	**4.87**	−1.14	**−1.94**	**−2.05**
Il3	NM_031513	Interleukin 3	**1.71**	1.35	1.09	**−2.67**
Il4	NM_201270	Interleukin 4	1.68	1.37	1.26	**−2.64**
Il6	NM_012589	Interleukin 6	**2.78**	−1.20	**−2.18**	**−3.81**
Inha	NM_012590	Inhibin α	**3.95**	−1.46	**−3.17**	**−3.03**
Inhba	NM_017128	Inhibin β-A	**5.67**	**−1.71**	−1.02	**−1.75**
Lefty1	NM_001109080	Left right determination factor 1	**2.48**	−1.08	**−1.95**	**−3.89**
Lep	NM_013076	Leptin	**4.15**	1.03	−1.14	**−2.67**
Lif	NM_022196	Leukemia inhibitory factor	**2.19**	**−2.58**	**−1.70**	**−3.20**
Mdk	NM_030859	Midkine	1.33	1.52	1.06	**−1.62**
Ngf	XM_227525	Nerve growth factor (β polypeptide)	1.44	1.11	**−1.51**	**−3.99**
Nodal	NM_001106394	Nodal homolog (mouse)	**1.68**	1.37	−1.00	**−2.64**
Tdgf1	XM_001056317	Teratocarcinoma-derived growth factor 1	**3.95**	**2.05**	1.01	**−3.43**
Tff1	NM_057129	Trefoil factor 1	**1.68**	1.37	−1.32	**−2.64**
Vegfa	NM_031836	Vascular endothelial growth factor A	1.25	**−2.34**	**−1.51**	−1.36

Multiple genes related to growth were evaluated for expression using real-time PCR via the RT^2 Profiler PCR Array system. The table lists the genes of interest evaluated and their fold increase or decrease in prostates obtained from TE-treated, TE/finasteride-treated, TE/RC-3940-II (25 μg/d)-treated, and TE/RC-3940-II (50 μg/d)-treated rats 42 d after the start of treatment with BN/GRP antagonist RC-3940-II. Data represent fold differences of individual gene expression between study groups TE-treated vs. control, TE-treated vs. TE/finasteride-treated, TE-treated vs. TE/RC-3940-II (25 μg/d)-treated, and TE-treated vs. TE/RC-3940-II (50 μg/d)-treated. Positive values indicate up-regulation of individual genes; negative values indicate down-regulation. Three experiments were run for each study group. The data were evaluated by two-tailed Student *t* test. Boldface depicts significant changes ($P < 0.05$).

Table S4. Expression of genes in rat prostates involved in inflammatory response after treatment with TE, TE and finasteride, or BN/GRP antagonist RC-3940-II

Gene	Accession no.	Description	Fold change			
			TE vs. control	TE/finasteride (0.07 mg/kg) vs. TE	TE/RC-3940-II (25 μg/d) vs. TE	TE/RC-3940-II (50 μg/d) vs. TE
Bcl6	NM_001107084	B-cell CLL/lymphoma 6	−1.05	−1.21	−1.16	**−1.73**
C3	NM_016994	Complement component 3	−1.40	**−2.40**	**−1.51**	−1.13
Casp1	NM_012762	Caspase 1	**1.55**	1.14	1.15	−1.34
Ccl11	NM_019205	Chemokine (C-C motif) ligand 11	**6.35**	**−1.90**	**−3.70**	**−1.84**
Ccl12	NM_001105822	Chemokine (C-C motif) ligand 12	**1.90**	**−2.67**	**−1.89**	**−3.95**
Ccl17	NM_057151	Chemokine (C-C motif) ligand 17	**2.74**	**1.55**	**−4.04**	**−2.22**
Ccl19	NM_001108661	Chemokine (C-C motif) ligand 19	−1.17	**−1.83**	**−2.88**	1.29
Ccl2	NM_031530	Chemokine (C-C motif) ligand 2	−1.23	−1.35	**−1.85**	**−1.88**
Ccl20	NM_019233	Chemokine (C-C motif) ligand 20	1.06	1.34	**−5.41**	−1.24
Ccl25	NM_001037203	Chemokine (C-C motif) ligand 25	−1.18	**−2.65**	**−2.44**	**−2.52**
Ccl3	NM_013025	Chemokine (C-C motif) ligand 3	**2.65**	1.51	**−3.83**	1.09
Ccl5	NM_031116	Chemokine (C-C motif) ligand 5	**2.21**	**−2.01**	−1.05	−1.45
Ccl6	NM_001004202	Chemokine (C-C motif) ligand 6	**1.80**	**−1.64**	−1.45	**−1.49**
Ccl7	NM_001007612	Chemokine (C-C motif) ligand 7	**2.60**	**−4.85**	**−3.31**	**−2.78**
Ccr1	NM_020542	Chemokine (C-C motif) receptor 1	**1.62**	**−2.43**	−1.39	**−3.49**
Ccr10	NM_001108836	Chemokine (C-C motif) receptor 10	**1.75**	**−1.96**	−1.29	**−2.82**
Ccr3	NM_053958	Chemokine (C-C motif) receptor 3	−1.19	−1.06	−1.25	**−2.16**
Ccr4	NM_133532	Chemokine (C-C motif) receptor 4	−1.19	−1.06	−1.25	**−2.87**
Ccr5	NM_053960	Chemokine (C-C motif) receptor 5	**1.79**	−2.36	**−2.46**	**−3.32**
Ccr6	NM_001013145	Chemokine (C-C motif) receptor 6	−1.12	**1.88**	**−2.84**	**−6.51**
Ccr7	NM_199489	Chemokine (C-C motif) receptor 7	3.96	−1.18	−1.52	**−2.63**
Cd40lg	NM_053353	CD40 ligand	−1.88	2.21	2.96	**−2.87**
Cx3cl1	NM_134455	Chemokine (C-X3-C motif) ligand 1	**2.11**	−1.64	−1.33	**−1.65**
Cx3cr1	NM_133534	Chemokine (C-X3-C motif) receptor 1	**3.83**	−1.41	−1.11	−1.42
Cxcl1	NM_030845	Chemokine (C-X-C motif) ligand 1 (melanoma growth-stimulating activity, α)	1.05	−1.25	**−1.94**	**−1.99**
Cxcl10	NM_139089	Chemokine (C-X-C motif) ligand 10	**2.46**	−1.50	1.36	**−1.64**
Cxcl11	NM_182952	Chemokine (C-X-C motif) ligand 11	**3.85**	**−1.98**	1.19	**−1.95**
Cxcl12	NM_022177	Chemokine (C-X-C motif) ligand 12 (stromal cell-derived factor 1)	−1.13	**−1.52**	1.16	**−1.88**
Cxcl3	NM_138522	Chemokine (C-X-C motif) ligand 3	−1.02	**−2.26**	**−3.78**	**−1.65**
Cxcl5	NM_022214	Chemokine (C-X-C motif) ligand 5	−1.11	−1.43	1.17	**−3.77**
Cxcl9	NM_145672	Chemokine (C-X-C motif) ligand 9	1.43	1.01	−1.28	**−2.56**
Cxcr3	NM_053415	Chemokine (C-X-C motif) receptor 3	**2.98**	**−1.73**	1.23	**−1.64**
Ifng	NM_138880	IFN-γ	−1.25	−1.06	−1.12	**−2.61**
Il10	NM_012854	Interleukin 10	**1.43**	**−19.74**	**−3.86**	−1.18
Il11	NM_133519	Interleukin 11	**1.69**	**−2.38**	−1.01	**−3.26**
Il13	NM_053828	Interleukin 13	−1.19	−1.06	−1.25	**−2.87**
Il13ra1	NM_145789	Interleukin 13 receptor, α1	**1.77**	−1.51	**−1.68**	**−2.35**
Il15	NM_013129	Interleukin 15	1.44	−1.50	−1.58	**−1.87**
Il17b	NM_053789	Interleukin 17B	6.26	2.10	−2.49	−3.93
Il1b	NM_031512	Interleukin 1β	**3.22**	**−3.22**	−1.29	**−1.95**
Il1f5	NM_001107814	Interleukin 1 family, member 5 (δ)	**1.98**	−1.29	−1.42	**−3.74**
Il1f6	NM_001106554	Interleukin 1 family, member 6	−1.19	**1.67**	−1.25	**−2.87**
Il1r1	NM_013123	Interleukin 1 receptor, type I	1.57	**−2.04**	−1.23	**−3.74**
Il6	NM_012589	Interleukin 6	**1.77**	−1.22	**−2.04**	**−2.46**
Il6r	NM_017020	Interleukin 6 receptor	1.59	−1.55	**−1.61**	**−2.18**
Il8ra	NM_019310	Interleukin 8 receptor, α	**1.90**	**−2.41**	**−2.84**	**−6.51**
Ptgs2	NM_017232	Prostaglandin-endoperoxide synthase 2	**1.93**	**−2.61**	−1.01	**−1.87**
Tnfrsf1a	NM_013091	Tumor necrosis factor receptor superfamily, member 1a	**1.86**	**−1.58**	−1.41	**−1.78**
Tollip	NM_001109668	Toll interacting protein	−1.03	1.14	−1.06	**−1.71**
Xcr1	NM_001106871	Chemokine (C motif) receptor 1	**4.31**	**−1.98**	**−6.44**	**−1.57**

Multiple genes involved in inflammatory response were evaluated for expression using real-time PCR via the RT^2 Profiler PCR Array system. The table lists the genes of interest evaluated and their fold increase or decrease in prostates obtained from TE-treated, TE/finasteride-treated, TE/RC-3940-II (25 μg/d)-treated, and TE/ RC-3940-II (50 μg/d)-treated rats 42 d after the start of treatment with BN/GRP antagonist RC-3940-II. Data represent fold differences of individual gene expression between study groups TE-treated vs. control, TE-treated vs. TE/finasteride-treated, TE-treated vs. TE/RC-3940-II (25 μg/d)-treated, and TE-treated vs. TE/RC-3940-II (50 μg/d)-treated. Positive values indicate up-regulation of individual genes; negative values indicate down-regulation. Three experiments were run for each study group. The data were evaluated by two-tailed Student *t* test. Boldface depicts significant changes ($P < 0.05$).

Table S5. Expression of genes in rat prostates involved in signal transduction after treatment with TE, TE and finasteride, or BN/GRP antagonist RC-3940-II

Gene	Accession no.	Description	Fold change			
			TE vs. control	TE/finasteride (0.07 mg/kg) vs. TE	TE/RC-3940-II (25 μg/d) vs. TE	TE/RC-3940-II (50 μg/d) vs. TE
Wnt pathway						
Birc5	NM_022274	Baculoviral IAP repeat-containing 5	**1.82**	**−2.14**	−1.16	**−1.49**
Vegfa	NM_031836	Vascular endothelial growth factor A	−1.01	**−1.53**	−1.21	**−1.48**
Wisp1	NM_031716	WNT1 inducible signaling pathway protein 1	−1.24	−1.01	1.30	**−2.57**
Hedgehog pathway						
Bmp2	NM_017178	Bone morphogenetic protein 2	−1.06	**−1.79**	1.13	**−1.77**
Foxa2	NM_01274	Forkhead box A2	**537.46**	**−599.45**	**−567.31**	**−1,076.40**
TGF-β pathway						
Cdkn1a	NM_080782	Cyclin-dependent kinase inhibitor 1A	1.27	−1.15	−1.04	**−1.50**
Cdkn2b	NM_130812	Cyclin-dependent kinase inhibitor 2B (p15, inhibits CDK4)	1.30	−1.38	−1.22	**−1.88**
NF-κβ pathway						
Cxcl1	NM_030845	Chemokine (C-X-C motif) ligand 1 (melanoma growth-stimulating activity, α)	−1.20	1.12	1.20	**−1.52**
Nos2	NM_012611	Nitric oxide synthase 2, inducible	−1.26	**2.45**	1.19	**−1.59**
Vcam1	NM_012889	Vascular cell adhesion molecule 1	**1.58**	**−1.77**	−1.26	**−1.41**
Jak–Stat pathway						
Irf1	NM_012591	IFN regulatory factor 1	1.30	**−1.57**	−1.13	**−1.40**
Mmp10	NM_133514	Matrix metallopeptidase 10	**3.56**	**−2.04**	**−1.94**	**−2.18**
LDL pathway						
Ccl2	NM_031530	Chemokine (C-C motif) ligand 2	**3.12**	−1.18	−1.16	**−1.83**
Sele	NM_138879	Selectin E	**2.18**	**−2.18**	**−2.69**	**−2.26**
Other signaling molecules						
Cd5	NM_019295	Cd5 molecule	**5.90**	**−12.71**	**−3.01**	**−3.63**
Mmp7	NM_012864	Matrix metallopeptidase 7	**2.48**	−1.56	**−2.66**	**−1.73**
Cyp19a1	NM_017085	Cytochrome P450, family 19, subfamily a, polypeptide 1, aromatase	−1.26	1.13	3.82	**−1.59**

Multiple genes involved in signal transduction were evaluated for expression using real-time PCR via the RT^2 Profiler PCR Array system. The table lists the genes of interest evaluated and their fold increase or decrease in prostates obtained from TE-treated, TE/finasteride-treated, TE/RC-3940-II (25 μg/d)-treated, and TE/RC-3940-II (50 μg/d)-treated rats 42 d after the start of treatment with BN/GRP antagonist RC-3940-II. Data represent fold differences of individual gene expression between study groups TE-treated vs. control, TE-treated vs. TE/finasteride-treated, TE-treated vs. TE/RC-3940-II (25 μg/d)-treated, and TE-treated vs. TE/ RC-3940-II (50 μg/d)-treated. Positive values indicate up-regulation of individual genes; negative values indicate down-regulation. Three experiments were run for each study group. The data were evaluated by two-tailed Student *t* test. Boldface depicts significant changes ($P < 0.05$).

Table S6. Oligonucleotide primers used for quantitative real-time RT-PCR

Gene	Accession no.	Forward (5′–3′)	Reverse (5′–3′)	Annealing temperature, °C
Human				
Grpr	NM_005314	CTACCCACTTTAAACCTC	TTTACTAAGAACTTTTGGC	57
Nmbr	NM_002511	CCTCAAACAGATGAATTACA	CTAATAATAGCAAGTGGTATGA	57
Brs3	NM_001727	TTTCAAGACCAAATCCAT	ACAAGTTAGCAGAAGTAA	57
Grp	NM_001012512	CTTGACTAAATTCGTGATT	GCATTAATTGGAAGACTC	57
Nmb	NM_205858	AGACACAGATTATGTTCCT	GTATGTAAAGAGCAAGGTT	57
Hprt	NM_000194	TCCATTCCTATGACTGTAGA	GATTATACTGCCTGACCAA	57
Rat				
Grpr	NM_012706	AACAACACCTTCAATCAA	GCAGGAATGACATAGATG	57
Nmbr	NM_012799	GGAGAATACAATGAACATACCA	CACAAACACCAGAACGAT	57
Brs3	NM_152845	TCTTGGTGTTCTACATTATCC	TTGTTCCTCAGTCGGTAT	57
Grp	NM_133570	ATTCTACTGGACCATCAA	TAGGTAGTTGTTCACAGA	57
Nmb	NM_001109149	CTCAAATGTGTTACTCTGT	CAGGGAAGCAAGAAATAC	57
Hprt	NM_012583	AGCGTCGTGATTAGTGAT	ATCTTCAGCATAATGATTAGGTA	55

Rat-specific primers were designed according to the following criteria: (*i*) a product size range of 70–180 bases; (*ii*) a primer size range of 18–24 bases; (*iii*) a temperature difference of 3 °C; and (*iv*) a GC content of 30–80%. The mRNA sequences used for the design of the primers were taken from the National Center for Biotechnology Information (NCBI) reference sequences. The primers were tested for sequence similarity to other genes with NCBI BLAST. The thermal cycling conditions for each set of primers comprised an initial denaturation step at 95 °C for 3 min and then 35–40 cycles of two-step PCR including 95 °C for 30 s and corresponding annealing temperature for 1 min. Data were collected during the annealing step and were analyzed further by the iCycler iQ Optical system software (Bio-Rad). Real-time PCR melting curve analyses revealed a single product for each primer set.

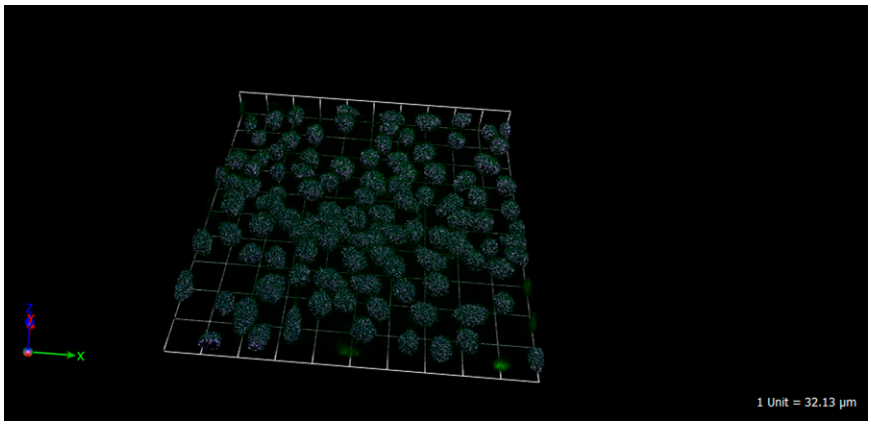

Movie S1. Representative confocal laser-scanning microscopy of control BPH-1 cells 6 h after start of the experiment. Cell volume of GRP-receptor–stained cells fixed with methanol was determined by 3D image analysis with a Zeiss LSM510/UV Axiovert 200M laser confocal microscope using Volocity imaging software. (Scale: 1 unit = 32.13 μm.)

Movie S1

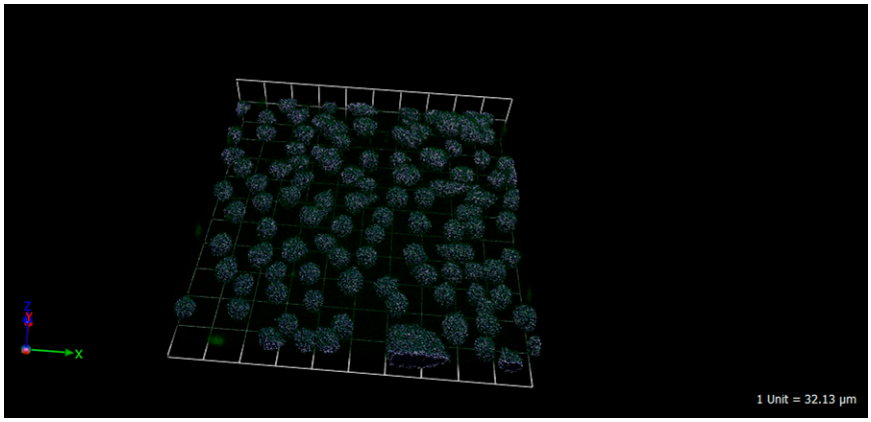

Movie S2. Representative confocal laser-scanning microscopy of BPH-1 cells treated with GRP antagonist RC-3940-II (10 μM) for 6 h. Cell volume of GRP-receptor–stained cells fixed with methanol was determined by 3D image analysis with a Zeiss LSM510/UV Axiovert 200M laser confocal microscope using Volocity imaging software. The findings indicate a 15.5% reduction in cell volume by RC-3940-II. (Scale: 1 unit = 32.13 μm.)

Movie S2

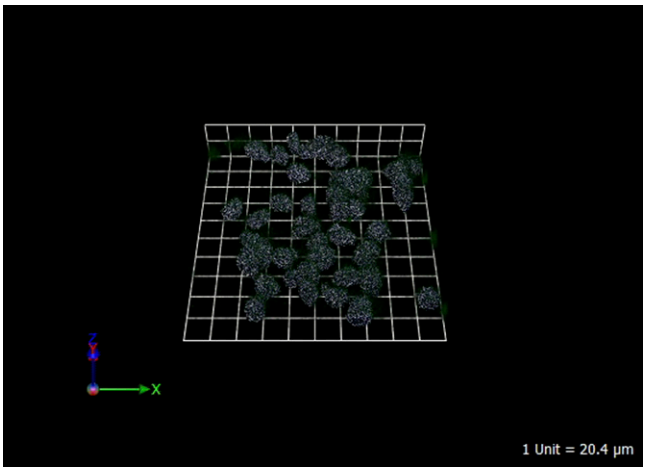

Movie S3. Representative confocal laser-scanning microscopy of control WPMY-1 cells 6 h after start of the experiment. Cell volume of GRP-receptor–stained cells fixed with methanol was determined by 3D image analysis with a Zeiss LSM510/UV Axiovert 200M laser confocal microscope using Volocity imaging software. (Scale: 1 unit = 20.4 μm.)

Movie S3

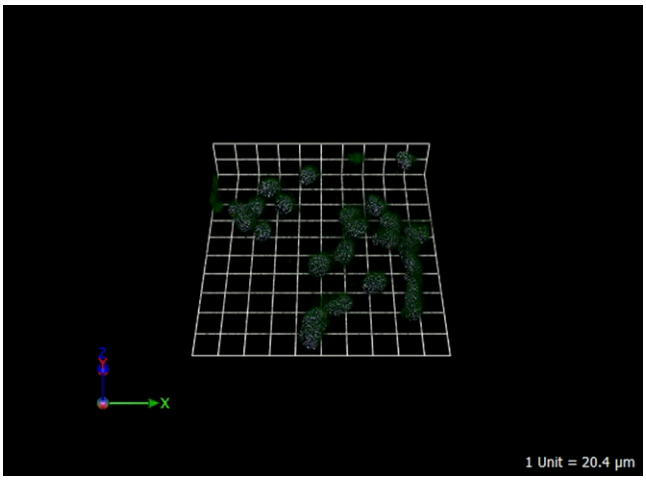

Movie S4. Representative confocal laser-scanning microscopy of WPMY-1 cells treated with GRP antagonist RC-3940-II (10 μM) for 6 h. Cell volume of GRP-receptor–stained cells fixed with methanol was determined by 3D image analysis with a Zeiss LSM510/UV Axiovert 200M laser confocal microscope using Volocity imaging software. The findings indicate a 15.6% reduction in cell volume by RC-3940-II. (Scale: 1 unit = 20.4 μm.)

Movie S4